Biomaterials 32 (2011) 3899–3909

Contents lists available at ScienceDirect

Biomaterials

journal homepage: www.elsevier.com/locate/biomaterials

# The biocompatibility and biofilm resistance of implant coatings based on hydrophilic polymer brushes conjugated with antimicrobial peptides

Guangzheng Gao [a,1], Dirk Lange [b,1], Kai Hilpert [c], Jason Kindrachuk [d], Yuquan Zou [a], John T.J. Cheng [e], Mehdi Kazemzadeh-Narbat [f], Kai Yu [a], Rizhi Wang [f], Suzana K. Straus [e], Donald E. Brooks [a,e], Ben H. Chew [b], Robert E.W. Hancock [d], Jayachandran N. Kizhakkedathu [a,e,*]

[a] Centre for Blood Research and the Department of Pathology and Laboratory Medicine, 2350 Health Sciences Mall, University of British Columbia, Vancouver, BC, Canada V6T 1Z3
[b] Department of Urological Sciences, University of British Columbia, Canada
[c] Institute of Functional Interfaces, Karlsruhe Institute of Technology (KIT), P.O. Box 3640, 76021 Karlsruhe, Germany
[d] Centre for Microbial Diseases and Immunity Research, Department of Microbiology and Immunology, University of British Columbia, 2259 Lower Mall Research Station, Vancouver, BC, Canada V6T 1Z4
[e] Department of Chemistry, University of British Columbia, Vancouver, BC, Canada V6T 1Z1
[f] Department of Materials Engineering, University of British Columbia, Vancouver, BC, Canada V6T 1Z4

ARTICLE INFO

*Article history:*
Received 21 January 2011
Accepted 9 February 2011
Available online 5 March 2011

*Keywords:*
Antimicrobial coatings
Implant-associated infection
Biofilm resistance
Blood/tissue toxicity
Antimicrobial peptides
Polymer brushes

ABSTRACT

Bacterial colonization on implant surfaces and subsequent infections are one of the most common reasons for the failure of many indwelling devices. Several approaches including antimicrobial and antibiotic-eluting coatings on implants have been attempted; however, none of these approaches succeed *in vivo*. Here we report a polymer brush based implant coating that is non-toxic, antimicrobial and biofilm resistant. These coating consists of covalently grafted hydrophilic polymer chains conjugated with an optimized series of antimicrobial peptides (AMPs). These tethered AMPs maintained excellent broad spectrum antimicrobial activity *in vitro* and *in vivo*. We found that this specially structured robust coating was extremely effective in resisting biofilm formation, and that the biofilm resistance depended on the nature of conjugated peptides. The coating had no toxicity to osteoblast-like cells and showed insignificant platelet activation and adhesion, and complement activation in human blood. Since such coatings can be applied to most currently used implant surfaces, our approach has significant potential for the development of infection-resistant implants.



## 1. Introduction

Bacterial infections associated with implanted devices pose a significant threat to patients and a serious challenge to clinicians [1–6]. High infection rates (2–6%) are observed for orthopaedic implants, dental devices, vascular grafts, urinary catheters, venous catheters [1,4–7] resulting in poor device performance in terms of safety and longevity. Biofilm formation on devices complicates treatments as biofilms are up to 1000-fold more antibiotic-resistant compared to planktonic bacteria [4,8]. Further, suboptimal exposure of antibiotics can promote the development of drug resistant phenotypes [9–12] and enhance biofilm formation [13]. Despite the fact that localized antimicrobial delivery through implant coatings is a promising approach [7,14–18], it is often beleaguered by the poor biocompatibility of such coatings [14,19]. Alternative, non-covalent coatings have the disadvantage of developing a concentration gradient from the implant surface, such that bacteria can respond to the antibiotic leading to the development of drug resistance [10,12].

Complex interactions between the pathogen, the implant device and the host are the origin of many device-associated infections [2,20]. Surface properties, including hydrophobicity or hydrophilicity, and the presence of surface charges, etc. play a major role in initial bacterial adhesion and proliferation [2,21]. Aside from this, surface interactions contribute to the host response at the surface of devices [20,22,23]. Thus the optimal design of an infection-resistant coating is very challenging as it must satisfy diverse requirements including optimal broad spectrum antimicrobial activity, protection against biofilm formation, and biocompatibility.

Here we describe the development of a specially structured infection-resistant coating on implants based on covalently grafted hydrophilic polymer brushes conjugated with an optimized series

* Corresponding author. Centre for Blood Research and the Department of Pathology and Laboratory Medicine, 2350 Health Sciences Mall, University of British Columbia, Vancouver, BC, Canada V6T 1Z3. Tel.: +1 604 822 7085; fax: +1 604 822 7742.
*E-mail address:* jay@pathology.ubc.ca (J.N. Kizhakkedathu).
[1] Contributed equally.

0142-9612/$ – see front matter © 2011 Elsevier Ltd. All rights reserved.
doi:10.1016/j.biomaterials.2011.02.013

of tethered antimicrobial peptides (AMPs). These AMPs, obtained through a high throughput screening method [24,25], showed broad spectrum activity against different pathogenic bacteria and yeast when immobilized on a surface [25]. AMPs are a logical alternative to conventional antibiotics due to their broad spectrum antimicrobial activities, including antibiotic-resistant and multi-drug resistant strains, limited induction of resistant phenotypes, and ability to selectively modulate the immune response of the host [26]. Covalently attached functional N-substituted polyacrylamide brushes on implant surfaces provide protection against non-specific interactions [27] and were used for one-end tethering of AMPs (Fig. 1). Surface concentrations of AMPs up to 5.9 μg/cm$^2$ were achieved. The polymer brush structure provided a flexible linker between the AMPs and the surface, reducing the influence of surface effects and confinement, which adversely affect peptide activity. Importantly, such coatings are robust and can be generated on most currently used biomedical materials including plastics, metals and ceramics providing a robust methodology for the generation of infection-resistant coatings.

## 2. Experimental

### 2.1. Materials

3-Amino propyl triethyoxysilane (APTES) (98%), 1, 1, 4, 7, 10, 10-hexamethyl triethylene tetramine (HMTETA) (97%), 2-chloropropionyl chloride (97%), methyl 2-chloropropionate (97%), CuCl (99%), $CuCl_2$ (99%) were purchased from Aldrich (Oakville, ON). *N*-(3-Aminopropyl) methacrylamide hydrochloride (APMA) (98%) and 3-maleimidopropionic acid *N*-hydroxysuccinimide ester (SMP) (97%) were from Polysciences, USA and were used as supplied. *N,N*-Dimethylacrylamide (DMA) (Aldrich, 99%) was distilled before use. Water purified using a Milli-Q Plus water purification system (DI water) (Milipore Corp., Bedford, MA) was used in all experiments. All other reagents were purchased from Aldrich and used without further purification. Single side polished silicon wafer (University Wafer, Boston, U.S.A.) deposited with titanium (~250 nm) was prepared by e-beam evaporation of titanium (physical vapor deposition). The process was progressed in a home-assembled Evaporator 2000 system equipped with a quartz crystal microbalance to monitor film thickness and a cryo-pump to reach high vacuum (~$10^{-7}$~$10^{-6}$ torr) conditions. After deposition, the substrates were washed with DI water, dried via $N_2$ gun, and stored for further usage. Cysteine containing peptides, were synthesized by GenScript Corp (~94% purity by HPLC) (NJ, USA) and were used as supplied. Ti wire (0.25 mm, 99.7%) and Quartz slides (76.2 × 25.4 × 1.0 mm) were purchased from Alfa Aesar, MA, USA.

### 2.2. Instrumentation

Absolute molecular weights of the polymers were determined by gel permeation chromatography (GPC) on a Waters 2690 separation module fitted with a DAWN EOS multi-angle laser light scattering (MALLS) detector from Wyatt Technology Corp (laser wavelength $\lambda = 690$ nm) and a refractive index (Optilab DSP) detector from Wyatt Technology Corp operated at $\lambda = 620$ nm. Aqueous 0.5 N $NaNO_3$ solution was used as the mobile phase at a flow rate of 0.8 mL/min. The dn/dc of Poly (*N,N*-dimethyacrylamide) (PDMA) and Poly N-(3-aminopropyl) methacrylamide (PAPMA) were determined to be 0.17 and 0.16 in a 0.5 N $NaNO_3$ solution. The dn/dc of the copolymers was calculated from the NMR composition data and dn/dc of individual homopolymers, and was used for the calculation of the molecular weight. The water used in all experiments was purified using a Milli-Q Plus water purification system (Millipore Corp., Bedford, MA). Dialysis was carried out using a Spectra/Pro dialysis membrane (MWCO 10000). $^1$H NMR spectra were recorded on a Bruker Avance 300 MHz NMR spectrometer using $D_2O$ as the solvent.

Attenuated Total Reflectance Fourier Transform Infrared (ATR-FTIR) spectra were recorded using a Thermo-Nicolet Nexus FTIR spectrometer with a MCT/A liquid nitrogen cooled detector, KBr beam splitter and MKII Golden Gate Single Refection ATR accessory (Specac Inc.). Spectra were recorded at 4 cm$^{-1}$ resolution and 256 scans were collected for each sample.

For static water contact angle measurements, digital images of a 2 μL water droplet on the surface were taken using a digital camera (Retiga 1300, Q-imaging Co.), and analyzed using Northern Eclipse software. Five different spots on the Ti-substrate were tested for each sample and the average value ± SD (standard deviation) is reported.

Dry polymer film thickness on the Ti deposited silicon wafer (Ti slides) surface was measured by ellipsometry. The variable-angle spectroscopic ellipsometry (VASE) spectra were collected on an M-2000 V spectroscopic ellipsometer (J.A. Woolham Co. Inc., Lincoln, NE) at 55°, 65°, and 75°, at wavelengths from 370 to 1000 nm with a M-2000 50Wquartz tungsten halogen light source. The VASE spectra were then fitted with a multilayer model on the basis of the WVASE32 analysis software, using the optical properties of a generalized Cauchy layer to obtain the "dry" thickness of the polymer layer.

Dry polymer film thickness on the Quartz slide surface was determined using atomic force microscopy (AFM) measurements in air. AFM used for this experiment was a commercially available multimode system with an atomic head of 50 × 50 μm$^2$ scan range which used a NanoScope IIIa controller (Digital Instruments, Santa Barbara, CA).

UV–Vis spectra were collected at room temperature in a Varian Cary 4000 spectrophotometer using a 1 cm path length quartz cell. SEM images were taken using Hitachi S4700 Scanning Electron Microscope.

### 2.3. Synthesis of peptide immobilized copolymer brushes on surface

Synthesis of peptide immobilized polymer layers involves i) surface immobilization of atom transfer radical polymerization (ATRP) initiator, ii) ATRP of DMA and APMA from the surface, and iii) maleimide functionalization of copolymer brushes followed by peptide conjugation (Scheme 1).

#### 2.3.1. Initiator modification of surface

The initiator modification was carried out in two steps: initial functionalization to generate amine groups followed by modification with 2-chloropropionyl chloride to generate atom transfer radical polymerization (ATRP) initiator groups on the Ti surface. The pre-treatment of Ti deposited silicon wafers (**Ti**) and the amine modification (**Ti-NH$_2$**) were carried out by following protocols reported in the literature to generate silane layers with thickness less than 2 nm [28]. The modified samples were dried in argon flow and stored under argon.

ATRP initiator modified surfaces were generated by treating with 2-chloropropionyl chloride. 2-chloropropionyl chloride (2.50 g, 19.68 mmol) and triethylamine (2.17 g, 21.40 mmol) were added dropwise to **Ti-NH$_2$** incubated in dichloromethane (DCM) (30 mL) at 0 °C over a period of 2 h. The reaction was

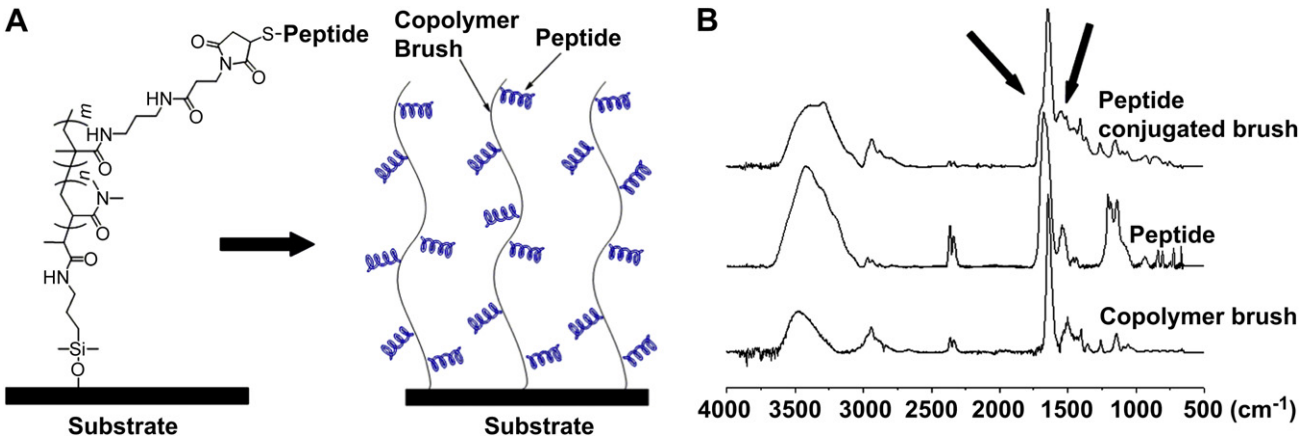


**Fig. 1.** [A] Representation of peptide immobilized copolymer brush on surface. [B] Comparison of ATR-FTIR spectra of peptide (Tet-20) immobilized copolymer brush on titanium surface with peptide alone and unmodified copolymer brush.

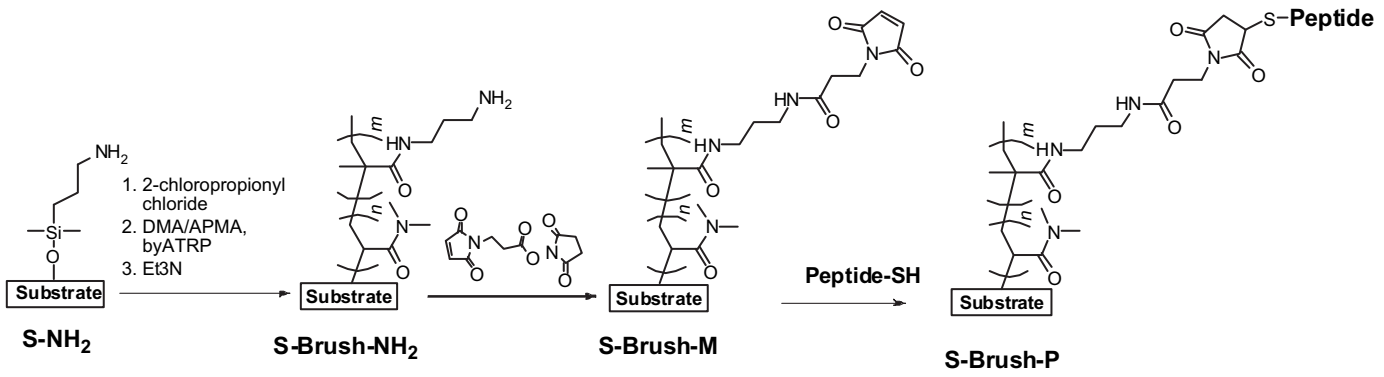


**Scheme 1.** Synthetic route for copolymer brushes and peptide conjugation.

continued at 0 °C for 4 h and left overnight at room temperature. The modified surfaces were cleaned by ultrasonication in DCM, acetone, methanol, and water consecutively, followed by drying and storage under argon flow. The dried ATRP initiator modified samples (**Ti**–**NH**–**Cl**) were characterized using X-ray photoelectron spectroscopy (XPS) and water contact angle measurements.

In the case of Ti-wire implants, the wire was entwined into implants that were approximately 1.0 × 1.0 × 0.3 $cm^3$ in size (Figure 3S). The amine modification procedure was similar to that used for Ti-slides [28] and was followed by ATRP initiator modification (**Ti-wire-Cl**). The samples were dried and stored under argon flow.

*2.3.2. Surface initiated ATRP of N,N-dimethylacrylamide and N-(3-aminopropyl) methacrylamide hydrochloride*

All the polymerization experiments were conducted in a glove box under argon atmosphere. For a typical experiment, DMA (0.5 g, 5 mmol) and APMA (0.18 g, 1 mmol) (ratio of DMA/APMA = 5) were dissolved in degassed purified water (4.5 mL). This solution was introduced into a $CuCl_2$ (0.5 mg, $3.7 \times 10^{-3}$ mmol), CuCl (3.7 mg, $3.7 \times 10^{-2}$ mmol) and HMTETA (22 μL, $8.1 \times 10^{-2}$ mmol) mixture, and stirred until homogeneous. Titanium slides modified with ATRP initiators (**Ti**–**NH**–**Cl**) were introduced to the polymerization mixture along with the addition of methyl 2-chloropropionate [4.3 μL (in 10% ethanol solution), $3.7 \times 10^{-3}$ mmol] and the polymerization was continued at 22 °C for 24 h. The polymerization was stopped by air exposure and followed by dilution with water. The resulting copolymer grafted Ti-slides were ultrasonicated in water two times (30 min each) and dried in a vacuum. The polymers formed along with the surface grafted polymer were dialyzed against water for 2 days (1000 MWCO membranes) and the copolymer was obtained by lyophilization. The monomer ratio was varied by changing the amount of DMA and APMA used for the reaction. The polymer grafted layer (Ti-Brush) was characterized using ATR-FTIR, ellipsometry and AFM measurements. A similar procedure was used for the synthesis of copolymer brushes on **Ti-wire-Cl** using a DMA/APMA ratio = 5/1. The molecular weight of the polymer was obtained using gel permeation chromatography with multiple angle light scattering (GPC-MALLS).

*2.3.3. Synthesis of maleimide group immobilized Ti surface*

Ti-Brush was immersed in 0.5 M $Et_3N$/water solution for 2 h at room temperature and ultrasonicated for 20 min to regenerate primary amine groups in the grafted copolymer chain. The surface was washed with water and ultrasonicated consecutively with water and methanol to produce primary amine functionalized brushes (**Ti-Brush-$NH_2$**). The primary amine functionalized surface was treated with 3-maleimidopropionic acid *N*-hydroxysuccinimide in acetonitrile solution (1 M solution) for 6 h at 22° C and ultrasonicated consecutively with acetonitrile and acetone, and dried. The maleimide functionalized surface (**Ti- Brush-M)** was characterized by ATR-FTIR and ellipsometry. A similar procedure was used for Ti-wire-Brush-M.

*2.3.4. Synthesis of peptide immobilized brushes*

The maleimide modified Ti surface was incubated with a solution of cysteine containing peptide Tet-213 in 100 mM sodium phosphate buffer (1 mg/ml) overnight followed by excess of 2-mercaptoethanol (0.1 g/mL) for another day. The peptide immobilized Ti slide was cleaned twice ultrasonically with water (15 min each) and the samples were dried in argon flow. The dried samples were stored under argon and characterized by ATR-FTIR, AFM, and ellipsometry. A similar procedure was used for the conjugation of other peptides (1010cys, Tet-20, Tet-21, Tet-26, HH2, MXX226) and for the Ti-Wire-Brush-M samples. The dried samples were stored at −20 °C under argon until antibacterial analysis. The samples were characterized by ATR-FTIR, water contact angle measurements, ellipsometry and AFM analysis.

*2.3.5. Peptide immobilized copolymer brush on quartz surface*

*2.3.5.1. Initiator modification.* Quartz slides (38.1 × 9.0 × 1.0 mm), cut from Quartz microscope slides (Alfa Aesar, 38.1 × 25.4 × 1.0 mm), were treated with Piranha solution at 70 °C for 4 h. The slides were washed with distilled water and dried via a stream of argon. The primary amine modified quartz slides were obtained by refluxing in 1% w/v (3-aminopropyl)trimethoxysilane/toluene solution. After 2 h, the slides were ultrasonicated consecutively with toluene, DCM, and dried via a stream of argon.

Amine modified quartz surfaces were treated with 2-chloropropionyl chloride (2.50 g, 19.68 mmol) and triethylamine (2.17 g, 21.4 mmol) in DCM (30 ml) at 0 °C over a period of 2 h. The reaction was continued at 0 °C for 4 h and left overnight at room temperature. The modified surfaces were cleaned by ultrasonication in DCM, acetone, methanol, and water consecutively, and preserved in argon after dried in vacuum.

*2.3.5.2. Surface initiated ATRP of N,N-dimethylacrylamide (DMA) and N-(3-aminopropyl) methacrylamide hydrochloride (APMA).* All the polymerization experiments were conducted in a glove box filled with Argon [29–31]. For a typical experiment, DMA (0.1 g, 1 mmol) and APMA (0.18 g, 1 mmol) were dissolved in degassed purified water (4.5 mL). This solution was introduced into $CuCl_2$ (0.5 mg, $3.7 \times 10^{-3}$ mmol), CuCl (3.7 mg, $3.7 \times 10^{-2}$ mmol), and hexamethyltriethylenetetramine (HMTETA) (22 μL, $8.1 \times 10^{-2}$ mmol) mixture, then stirred until homogeneous. Quartz slides modified with ATRP initiators (**Q**–**NH**–**Cl**) were introduced into the polymerization mixture along with the addition of methyl 2-chloropropionate [4.3 μL (in 10% ethanol solution), $3.7 \times 10^{-3}$ mmol] and the polymerization was continued at 22 °C for 24 h. The polymerization was stopped by air exposure followed by dilution with water. The resulting copolymer grafted quartz slide was ultrasonicated in water two times (15 min each) and dried in a vacuum. The polymer in solution and the surface grafted polymer were dialyzed against water for 2 days (MWCO 1000 membranes) and the polymer was obtained by lyophilization. The polymer was characterized using GPC-MALLS. Dry thickness of the polymer brush was measured by AFM.

The graft density of the polymer layer was calculated using the following equation

$$h_b = \frac{\sigma_b}{\rho_b \times N_A} \times M_{nb}$$

[$\sigma_b$: graft density, $M_{nb}$: number average molecular weight of grafted chains, $h_b$: polymer layer thickness, $\rho_b$: density of copolymer (1.20 g/mL) [32,33] $N_A$: Avogadro's number.]

*2.3.5.3. Peptide conjugation onto quartz surface*

*2.3.5.3.1. Maleimide group conjugation.* Initially the copolymer brush conjugated quartz slides were washed with aqueous 0.5 M $Et_3N$ (20 mL) for 20 min. The surface was then washed with water and ultrasonicated consecutively with water, and methanol, and dried. The surface was treated with 3-maleimidopropionic acid *N*-hydroxysuccinimide (1 M solution, 4 mL) in acetonitrile for 6 h at 22° C, ultrasonicated consecutively with acetonitrile and acetone, and dried.

*2.3.5.3.2. Peptide conjugation.* Modified quartz slides from the previous step were treated with a solution of cysteinylated Tet-20 (Tet20cys) (KRWRIRVRVIRKC) (1 mg/ml, 10 mL) in 0.1 M sodium phosphate buffer overnight followed by excess 2-mercaptoethanol (0.1 g/mL) for another day. The peptide immobilized quartz slides were ultrasonically cleaned twice in water (15 min each) and dried in an argon flow. The dried samples were stored under argon and characterized by UV–Vis spectroscopy and AFM analysis. The amine saturation and peptides/chain were calculated from the brush thickness increase measured using AFM analysis after Tet20cys conjugation. The peptide density on the surface was calculated from the thickness of the brush before and after peptide conjugation, amount of polymer grafted, molecular weight and graft density values (see supporting information).

### 2.4. Antibacterial analysis

#### 2.4.1. Antimicrobial activity of peptide immobilized Ti-slides

Peptide immobilized polymer brush coated and bare Ti-slides were each placed in a well of a 24-well microtiter plate. The samples were then sterilized with 300 μl of 70% ethanol for 5 min. The ethanol solution was subsequently removed after every 5 min and the sterilization was repeated 5 times. The samples were then equilibrated 5 times with 300 μl of 1X BM2 culture media. 200 μl of *Pseudomonas aeruginosa* PA01 expressing a luciferase gene cassette (*luxCDABE)* was added to each well that contained a titanium sample. This enables for bacterial quantification using luminescence. The microtiter plate was then placed on a shaker at the speed of 190 rpm to provide a homogenous liquid environment for the interaction. Incubation was done at 37 °C for 4 h. The bacterial culture was then transferred to a 96-well TECAN® plate and the luminescence emission was measured using a TECAN® Spectrafluor Plus spectrometer (TECAN U.S., Inc.). A decrease in the luminescence reading is directly related to the inhibition of the bacterial growth which has previously been confirmed by bacteria colony count measurements [25].

The luminescence inhibition rate of the examined sample was calculated by equation.

$$R_p = \frac{(I_c - I_p)}{I_c} \times 100\%$$

($R_p$: Inhibition of Luminescence, $I_c$: Average luminescence of control sample (pure Ti slide), $I_p$: Average luminescence of peptide immobilized Ti slide).

#### 2.4.2. Antimicrobial activity of peptide immobilized Ti-wire implants

Peptide immobilized polymer brush coated and bare Ti-wire implants were placed each in a well of a 24-well microtiter plate. The wires were then sterilized with 300 μL of 70% ethanol each. The ethanol solution was removed after 5 min and the sterilization was repeated 5 times. The titanium wires were then rinsed 5 times using 300 μL of BM2 culture media. 200 μL of the *P. aeruginosa* PA01 *lux* strain culture was added at a designated concentration to each well that contained a titanium sample. The microtiter plate was then placed on a shaker at the speed of 190 rounds per minute to provide a homogenous liquid environment for the interaction. Following incubation at 37 °C for 4 h, the bacterial culture was transferred to a new microtiter plate and serially diluted with BM2 medium and enumerated using CFU counts. Each dilution was plated in triplicate on a Mueller Hinton agar plate and incubated at 37 °C for 24 h. The number of colony forming units (CFU) at each dilution rate was counted after incubation and the average CFU/ml was determined [25]. A similar procedure was used for the testing antimicrobial activity against *Staphylococcus aureus*.

#### 2.4.3. SEM analysis of bacteria incubated Ti-wire samples

For SEM analysis, the bacteria incubated Ti-wire implants were washed three times with 0.1 M PBS solution and fixed in 2.5% glutaraldehyde in 0.1 M PBS for 2 h at 4°C. After washing the samples 3 times with 0.1 M PBS, the specimens were dehydrated using graded ethanol (10 min each of 50, 70, 80, 90 and 100%) and dried. Samples were viewed using a Hitachi S4700 Scanning Electron Microscope.

### 2.5. Determination of biofilm formation

For this assay *P. aeruginosa* ATCC 27853 was used. An overnight culture was diluted 1:10 in 1/4 Brain Heart Infusion (BHI) Broth to obtain $10^8$ CFU/ml, and transferred to sterile 15 ml tubes to which either a Ti-slide conjugated with peptides (from Section 2.3) or bare Ti slide or Ti slide with copolymer brush without peptides was added. The tubes were mounted in an overhead shaker (Enviro Genie by Scientific Industries Inc.) and incubated at 37 °C at 6.12 rpm. Initial screen was performed for 1, 2, 3 and 7 days. Since the protective effect of the peptide coated titanium slides was still observed after 7 days, subsequent experiments were performed over a period of 7 days. After incubation the Ti-slides were washed for 5 s in washing buffer (10 mM Tris, 5 mM Magnesium acetate, pH 8.0), and stained with SYTO 9 (Invitrogen) according to the manufactures protocol. The images were taken using an Axioplan 2 Imaging unit (Carl Zeiss). For quantification of the biofilm, the Ti-slides were divided into 12 sectors, and for each sector 1 image was taken. Five representative images were chosen and each image was divided into 15 sectors for which the bacteria were counted.

### 2.6. In vivo testing of Tet-20 coated implants in rats

To test the ability of the peptide coated titanium implants to kill bacteria and inhibit infection, the wires were implanted into pockets made on the dorsal side of the rats and challenged with $10^8$ CFU *S. aureus*. The study protocol was approved by the University Animal Ethics Committee and carried out under the Canadian Council on Animal Care guidelines. Female Sprague–Dawley rats ($n = 14$) weighing between 200 g– 250g were housed with water and food available *ad libidum*. Following a mandatory 5 day acclimation period, the dorsal aspect of each animal was implanted with the Ti-wire implant conjugated with Tet-20 (from Section 2.3) (right side) or PDMA brush coated control implants (left side). Implantation was carried out under general anesthesia using isofluorane. The animals were positioned prone and the hair was shaved on the dorsal side just below the shoulder. A 0.5 mm incision was made, and a subcutaneous pocket was bluntly created using a hemostat. The implants were placed into the subcutaneous pocket at which point 250 μl of approximately $10^8$ bacteria was injected onto the surface of the implant. The wound was closed using 5/0 vicryl sutures.

After 7 days, the animals were sacrificed using $CO_2$ asphyxiation and the wounds were opened to remove the implants. The implants were washed in sterile phosphate buffered saline (PBS) to remove non-adhered bacteria. To remove adherent bacteria, the implants were placed in fresh PBS and sonicated for 10 min using a sonication water bath (Aquasonic Model 50T, VWR). The solutions were serially diluted and the numbers of bacteria were enumerated using CFU counts.

### 2.7. Platelet activation and adhesion

Peptide immobilized Ti-wire implants, PDMA brush coated Ti-wire implants without peptides and bare Ti-wire implants were used for this study. Platelet activation characterized by flow cytometry and adhesion was determined using SEM analysis. Fresh human blood anticoagulated with sodium citrate (1:9) was centrifuged at 193 × g (Allegra X-22R Cengtrifuge, Beckman Coulter) for 12 min to obtain platelet rich plasma (PRP).

The Ti-wires (bare and peptide immobilized) were incubated with 700 μl of PRP in 1.5 mL polystyrene tubes (Eppendorff) at 37 °C. After 1 h incubation, 5 μL of the incubation mixture was removed and mixed with 40 ul PBS buffer pH 7.4 and 5 μl of monoclonal anti-CD42a-FITC (FITC: fluorescein isothiocyanate to recognize the platelet population) or 5 μL of monoclonal anti-CD62P-PE (p-selectin marker, PE: phycoerythrin) for 30 min (final incubation volume 50 ul). Following addition of the antibodies, the samples were incubated in the dark at 37 °C for 1 h. Samples were withdrawn after 3 h and tested as described above.

As a positive control for platelet activation, 5 ul of PRP were mixed with 30 ul PBS buffer, 5 ul of GPRP, 5 ul of CD62-PE and 5 ul of bovine thrombin (Sigma). Mouse IgG PE (5 uL), was used as the non-specific binding control for CD62PE antibody. Mouse IgG FITC (5 uL), was used as the non-specific binding control for CD42FITC antibody. Platelet activation was measured using a flow cytometer (BD FACS Canto II) after fixing the platelets using 1 ml of formal saline. Since CD42a is a platelet marker that is independent of activation status, the level of platelet activation is reported as a percentage of anti-CD62P-PE by counting 10,000 platelets for each sample. All experiments were performed in duplicate, following 1 h and 3 h incubation in a 37 °C water bath. Average ± SD values from three different donors are reported.

For SEM analysis, titanium samples incubated in platelet rich plasma were washed three times with 0.1 M PBS followed by incubation in 2.5% glutaraldehyde in 0.1 M PBS for 2 h at 4°C. After washing the samples 3 times with 0.1 M PBS, the specimens were dehydrated using graded ethanol (10 min each of 50, 70, 80, 90 and 100%) and dried. Samples were viewed using a Hitachi S4700 Scanning Electron Microscope. The adhered platelets were counted from images randomly taken from different parts of the specimen.

### 2.8. Complement activation analysis

A modified hemolytic assay that measures the amount of residual complement content of titanium-treated human serum was performed to analyze the level of complement activation by the titanium samples using antibody-sensitized sheep erythrocytes. Two incubation steps were utilized. First, all titanium wire samples were incubated and reacted with 20% human serum (diluted in $GVB^{2+}$), followed by incubation with antibody-sensitized sheep RBC (EA cells) in order to measure the amount of complement activity remaining.

A total of 2 mL of 20% human serum was added to each sample and incubated for 1 h at 37 °C. Untreated 20% human serum incubated under the same conditions served as the complete lysis control. Similarly, heat aggregated IgG (final concentration 5 mg/mL) and EDTA (final concentration 10 mM) were incubated with 20% human serum for 1 h at 37 °C and served as the positive and negative control. Following the initial incubation period, 50 μL of the treated serum samples were diluted with two volumes of $GVB^{2+}$. Equal volumes of the diluted serum samples were then added to tubes containing EA cells (75 μL). Tubes contained either 75 μL EA cells and $GVB^{2+}$ buffer alone served as the EA color control. All tubes were then incubated 1 h at 37 °C and the reaction was stopped by the addition of 0.3 mL of GVB-EDTA. Intact EA cells were spun down and the supernatants were sampled. The amount of complement activity remaining in each tube was compared with that of serum incubated with buffer only (100% EA lysis).

The percentage EA lysis was calculated using average absorbance values as follow:

$$\%\text{EA lysis} = \left(OD_{540,\ \text{test sample}} - OD_{540,\ \text{color control}}\right) \Big/ \left(OD_{540,\ 100\%\ \text{lysis}} - OD_{540,\ \text{color control}}\right) \times 100.$$

Percentage of complement activation by the titanium samples was expressed as: 100%−% EA lysis. Serum from three different donors was tested and the average ± SD values are reported.

### 2.9. MG-63 cell-proliferation/adhesion analysis

Commercially available osteoblast-like cells from human osteosarcoma (MG-63, ATCC® CRL-1427™, USA) were cultured in a 12-well plate in Dulbecco's modified eagle medium supplemented with 10% fetal bovine serum and 1% penicillin/streptomycin. Cells were cultured under standard conditions at 37 °C in a humidified atmosphere containing 5% $CO_2$ at passage 9 with the culturing medium renewed every two days. The growth and viability of cells colonizing the samples was evaluated by measuring the mitochondrial dehydrogenase activity using a modified MTT (3-(4,5-dimetyl-2-tiazolyl)-2,5-diphenyl-2H-tetrazolium bromide) (Biotium Inc., USA) reduction assay. For SEM analysis of cell adsorption on titanium wire, the samples were washed with 0.1 M PBS for three times and incubated in 2.5% glutaraldehyde in 0.1 M PBS for 2 h at 4°C. After washing the samples for 3 times with 0.1 M PBS, post fixation is done with 1% Osmium tetroxide ($O_5O_4$) in PBS for 2 h at 4°C. Then specimens were dehydrated using graded ethanol (10 min each of 50, 70, 80, 90 and 100%) and dried. The samples were subsequently critically point dried and Pt/Au sputter coated. Samples were viewed using a Hitachi S4700 Scanning Electron Microscope. The number of adhered cells were counted by taking images randomly from five different spots on the specimen and the average value ± SD is reported.

### 2.10. Atomic force microscopy force measurements

Atomic force microscopy (AFM) measurements were performed on a multimode, Nanoscope IIIa controller (Digital Instruments, Santa Barbara, CA) equipped with an atomic head of 130 × 130 μm$^2$ scan range. AFM measurements were performed underwater in contact mode using a commercially manufactured V-shaped silicon nitride ($Si_3N_4$) cantilever with gold on the back for laser beam reflection (Veeco, NP-S20). The spring constant of the AFM cantilever was measured using the thermal equipartition theorem [34,35]. Force measurements were performed on this instrument using a fluid cell modified to allow temperature adjustment and measurement. The experiments were performed underwater in force mode. On tip approach the onset of the region of constant compliance was used to determine the zero distance, and on retraction the region in which force was unchanged was used to determine the zero force. The rate of tip-sample approach or retraction was typically 1 μm/s but ranged between 0.05 and 5 μm/s.

The raw AFM force data (cantilever deflection vs. displacement data) were converted into force vs. separation following the principle of Ducker et al. by using custom Matlab v.5.3 (Math Works, Natick, MA) software [36]. The software converts the cantilever deflection vs. linear voltage displacement transformer signal into restoring force vs. tip-substrate separation using user input trigger and spring constant values. We followed our published protocol for the calculation of the adhesive force [33]. Average value ± SD from 50 different force curves from different spots on the substrate are reported. Typical force-distance curves are given in Figure 1S.

### 2.11. Circular Dichorism (CD) spectroscopy analysis of surface immobilized Tet-20

Circular Dichorism (CD) spectroscopy analysis of surface immobilized Tet-20 were measured with a Jasco J-800 spectropolarimeter and 1 cm path length quartz cell for quartz surface samples and 0.2 cm path length quartz cell for solution samples. Surface CD and UV–vis spectra (Varian Cary 4000 spectrophotometer) of Tet-20 immobilized Quartz slide were measured by putting the samples Quartz slide (38.1 × 9.0 × 1.0 mm) in a 1 cm quartz cell.

Solution CD samples with a constant peptide concentration of 0.2 mM were prepared in 1:100 peptide to lipid (P/L) molar ratios, using 1:1 M lipid mixtures of DMPC/DMPG. Appropriate amounts of lipids in chloroform were dried using a stream of nitrogen gas to remove most of the chloroform and vacuum dried overnight in a 5 ml round bottom flask. After adding 450 μl of PBS and 0.1 umol of peptide in PBS(50 μl) to the dried lipids, the mixture was sonicated in a water bath for a minimum of 30 min (until the solution was no longer turbid) to ensure lipid vesicle formation. For all samples, corresponding background samples without peptides were prepared for spectral subtraction.

CD analysis of Surface immobilized peptide samples were performed in a similar fashion. A constant lipid concentration of 1.0 mM was prepared using 1:1 M lipid mixtures of DMPC/DMPG in a 5.0 ml round bottom flask. After vacuum-drying, 1.5 ml of PBS was added to the dried lipids and the mixture was sonicated as described above. Then, the lipid solution was pipetted into the quartz cell. Corresponding background samples were run initially without placing the sample quartz slide in the quartz cell.

Solution and surface CD experiments were carried out using a JASCO J-810 spectropolarimeter (Victoria, BC) at 30°C. Briefly, the spectra were obtained over a wavelength range of 190–250 nm, using continuous scanning mode with a response of 1 s with 0.5-nm steps, a bandwidth of 1.5 nm, and a scan speed of 50 nm/min. The signal/noise ratio was increased by acquiring each spectrum over an average of three scans. Finally, each spectrum was corrected by subtracting the background from the sample spectrum. Solution CD samples were placed in a cell (0.1 cm in length) in 200 uL portions, while the peptide immobilized quartz slides (as described above) were directly placed in the quartz cell for the CD analysis and then in the sample compartment. The temperature of the sample compartment was kept constant by means of a water bath.

To examine the % structure content of Tet20cys and surface tethered Tet20cys in different environments, all spectra were fitted using three different programs (CDSSTR, CONTINLL, and SELCON3).

## 3. Results and discussion

We first investigated the development of primary amine functionalized copolymer brushes containing *N,N*-dimethylacrylamide (DMA) and aminopropyl methacrylamide hydrochloride (APMA) (Scheme 1,) using aqueous surface initiated atom transfer radical polymerization. A titanium deposited silicon wafer was used as a model surface for the optimization of surface chemistry, and for the determination of the polymerization conditions and polymer brush properties (Table 1). This was later adapted to various materials (Table 2).

We hypothesized that a high surface concentration of AMPs could be achieved by conjugating the peptides to surface immobilized primary amine functionalized polymer chains. To test this hypothesis, the AMP Tet-213 (Table 2) was labeled C-terminally with a cysteine and conjugated onto copolymer brushes on Ti-slides (Fig. 1A, Scheme 1). Primary amine groups were modified with a bifunctional 3-maleimidopropionic acid *N*-hydroxysuccinimide ester to generate maleimide functionalized copolymer brushes followed by a selective and specific reaction of maleimide groups to thiol groups on cysteine functionalized AMPs. The composition, graft density and molecular weight of the copolymer brushes were optimized to yield high peptide density (Fig. 2). Brush composition, PDMA/PAPMA (5/1), resulted in high peptide density for AMP Tet-213. Surface attachment was confirmed by i) the presence of specific absorption peaks for the peptide in attenuated total reflectance Fourier Transform Infra Red (ATR-FTIR) spectrum (Fig. 1B) of peptide conjugated brush, ii) the measured increase in dry thickness of the brush layer after peptide conjugation and iii) the increase in water contact angle from 42.1° to 65.4°, following peptide conjugation (Table 2). From the increase in dry thickness of the polymer grafted layer upon peptide conjugation (Figure 2S, supplementary information), the peptide density on the surface was calculated to be 14.5

**Table 1**
Effect of monomer composition on PDMA-*co*-APMA grafting on Ti surface[a]

| Sample | $[DMA]_0/[APMA]_0$ | $M_n$[b] ($\times 10^{-4}$) | $M_w/M_n$[b] | Dry Thickness $h_b$[c] (nm) | Graft Density[d] (chains/nm$^2$) ($\times 10^2$) |
|---|---|---|---|---|---|
| Ti-1C | 2/1 | 17.02 | 1.16 | 40.7 ± 2.0 | 18.0 ± 0.8 |
| Ti-2C | 3/1 | 14.86 | 1.29 | 31.2 ± 3.2 | 15.3 ± 1.4 |
| Ti-3C | 4/1 | 16.71 | 1.49 | 35.8 ± 1.5 | 15.7 ± 0.6 |
| Ti-4C | 5/1 | 13.93 | 1.47 | 30.9 ± 1.1 | 16.1 ± 0.6 |
| Ti-5C | 10/1 | 16.35 | 1.45 | 48.0 ± 1.5 | 21.4 ± 0.6 |
| Ti-PD | 1/0 | 70.99 | 1.46 | 428.7 ± 24.1 | 43.6 ± 2.2 |

[a] Condition: $[HMTETA]_0/[CuCl]_0/[CuCl_2]_0/[I]_0/([DMA]_0 + [APMA]_0) = 2.2/1/0.1/0.1/156$, $[DMA]_0 + [APMA]_0 = 1.2$ mol/L, r.t., 24 h.
[b] Determined by GPC.
[c] Surface copolymer brush thickness, determined by ellipsometry.
[d] Calculated from brush thickness and $M_n$.

**Table 2**
Characteristics of the antimicrobial peptide conjugated surface.

| Substrate | Antimicrobial peptide | Sequence | Brush thickness (nm)[d] | | Peptide density (peptides/nm$^2$)[f] | Peptide weight (μg/cm$^2$)[f] | Water contact angle (deg)[h] |
|---|---|---|---|---|---|---|---|
| | | | Before | After | | | |
| Ti slide[a] | Tet-213 | KRWWKWWRRC | 30.9 ± 1.1 | 70.1 ± 1.6 | 14.5 ± 0.6 | 3.8 ± 0.2 | 65.4 ± 1.7 |
| | 1010cys | IRWRIRVWVRRIC | | 73.8 ± 2.1 | 14.2 ± 0.7 | 4.3 ± 0.2 | 43.4 ± 4.7 |
| | Tet-20 | KRWRIRVRVIRKC | | 63.8 ± 0.9 | 10.2 ± 0.3 | 3.1 ± 0.1 | 51.5 ± 0.8 |
| | Tet-21 | KKWKIVVIKWKKC | | 64.7 ± 1.3 | 11.2 ± 0.4 | 3.1 ± 0.1 | 45.8 ± 1.2 |
| | Tet-26 | WIVVIWRRKRRRC | | 65.1 ± 1.2 | 10.5 ± 0.4 | 3.2 ± 0.1 | 37.2 ± 1.3 |
| | HH2 | VNLRIRVAVIRAC | | 86.8 ± 2.5 | 23.9 ± 1.1 | 5.9 ± 0.3 | 73.3 ± 1.7 |
| | MXX226 | ILRWPWWPWRRKC | | 81.8 ± 1.9 | 16.9 ± 0.6 | 5.3 ± 0.2 | 66.3 ± 1.5 |
| Ti wire[b] | Tet-20 | | -[i] | -[i] | 19.0 ± 1.6[g] | 5.6 ± 0.5 | -[i] |
| Quartz (Q-1-1)[c] | Tet-20 | | 35.4 ± 1.1[e] | 73.2 ± 1.8[e] | 11.6 ± 0.3 | 3.4 ± 0.1 | -[i] |

[a] Peptide immobilized copolymer brush (DMA/APMA) on titanium deposited silicon wafer, copolymer composition (DMA/APMA molar ratio) = 5/1; copolymer brush molecular weight ($M_n$) = 13.93 × 10$^4$, $M_w/M_n$ = 1.47, grafting density of brush = 0.16 chains/nm$^2$.
[b] Peptide (Tet-20) immobilized copolymer brush on titanium wire (Alfa Aesar, 99.7%) (diameter = 0.25 mm, surface area = ~20 cm$^2$), copolymer composition (DMA/APMA molar ratio) = 5/1; copolymer brush molecular weight ($M_n$) = 15.44 × 10$^4$, $M_w/M_n$ = 1.53, brush grafting density = 0.21 chains/nm$^2$.
[c] Peptide (Tet-20) immobilized copolymer brush on quartz slide (Alfa Aesar), copolymer composition (DMA/APMA molar ratio) = 1/1; copolymer brush molecular weight ($M_n$): 11.50 × 10$^{-4}$, $M_w/M_n$: 1.39, brush grafting density: 0.18 chains/nm$^2$.
[d] Determined by ellipsometry before and after peptide conjugation.
[e] Determined from atomic force microscopy measurements.
[f] Calculated from brush thickness or weight increase after peptide conjugation (see supplementary information).
[g] Calculated from the amount peptide grafted after cleaving the polymer from the surface.
[h] Water contact angle of DMA/APMA copolymer brush before modification = 42.1 ± 1.3°.
[i] Not determined.

peptides/nm$^2$, which is considerably higher than the density observed after direct surface conjugation of peptide onto Ti surfaces (1–4 peptide/nm$^2$) [37]. Other AMPs (Table 2) were also conjugated to a Ti surface using the same chemistry. Copolymer brush properties such as molecular weight, polydispersity, graft density and composition were kept constant. A range of peptide densities on the surface, varying from 10 to 24 peptides/nm$^2$, was obtained with various peptides (Table 2). Water contact angles ranged between 37° to 73° depending on the peptide and its density on the surface. The water contact angle on the surface was more influenced by the structure of the peptides than their graft density (Table 2).

To investigate the antimicrobial activity of the tethered AMPs within the polymer brush, a previously-developed luminescence screening method [24,25], using *P. aeruginosa* strain H1001 that expresses a luciferase gene, was used. Briefly, light production

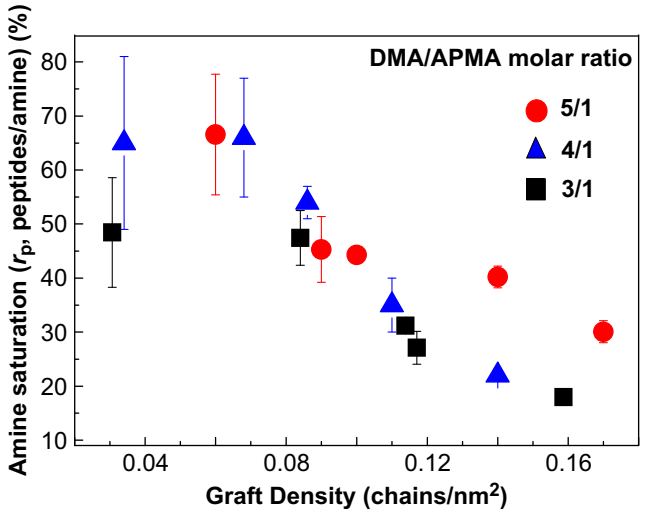


**Fig. 2.** Effect of copolymer graft density and composition of brushes on peptide conjugation (Tet-213 is used as an example). PDMA/P(APMA) composition (5:1) generated maximum peptide grafting density on the surface compared to other copolymer compositions.

requires metabolic energy from the bacterium, hence the inhibition of luminescence (IL $IL_{50}$ or $IL_{100}$- represents 50% or 100% bacterial killing respectively) indicates disturbance of metabolism. It was previously confirmed that the $IL_{50}$ or $IL_{100}$ is correlated with a decrease in bacterial viability by bacterial colony counts [24,25]. Different surface tethered peptides showed different inhibition levels of bacterial luminescence production, with IL values approaching 100% in some cases (Fig. 3A), confirming that the strong direct antimicrobial activities of AMPs are retained following polymer brush immobilization.

A peptide, Tet-20, that gave an excellent IL values close to 100% against *P. aeruginosa* strain PA01 was selected and conjugated on Ti-wire (Table 2 & Figure 3S in supplementary information). The molecular weight properties of the grafted copolymer chains were unambiguously determined using gel permeation chromatography analyzed by multi-angle light scattering after cleavage from the surface (Table 2). The amount of peptide conjugated to the copolymer brush on Ti-wire was determined using thermogravimetric analysis (TGA): approximately 19 Tet-20 peptide molecules per nm$^2$ were conjugated onto the copolymer brush on Ti-wire. We further evaluated the antimicrobial activity of Tet-20 coated Ti-wires *in vitro* against both Gram-negative and Gram-positive bacterial strains, *P. aeruginosa* and *S. aureus*. Ti-wires were incubated with the bacteria (1–5 × 10$^5$ CFU/ml) for 4 h at 37 °C. Samples were taken at one and 4 h, the bacteria were diluted, plated on agar plates and the colony forming units (CFU) were counted. Tet-20 immobilized Ti-wire implants showed a 5 log decrease in CFU compared to Ti-wires (Fig. 3B,C) and copolymer brush coated Ti-wires without peptides; no survivors were detected within the first hour (Fig. 3B,C) (see also Figure 4S, supplementary information). These results confirmed the antimicrobial activity of AMP-tethered polymer brush coating on Ti-wires *in vitro*.

Another critical property for implants is the retention of antimicrobial activity over the long term to prevent biofilm formation. Ti-slides with different tethered AMPs (Tet-20, Tet-26, Tet-213 and 1010) were selected to study the inhibitory effects on bacterial biofilm development, using *P. aeruginosa* ATCC 27853. An overnight culture was diluted 1:10 in 1/4 Brain Heart Infusion (BHI) Broth to obtain 10$^8$ CFU/ml, and transferred in sterile 15 ml tubes containing the Ti-slides. The tubes were mounted in an overhead shaker

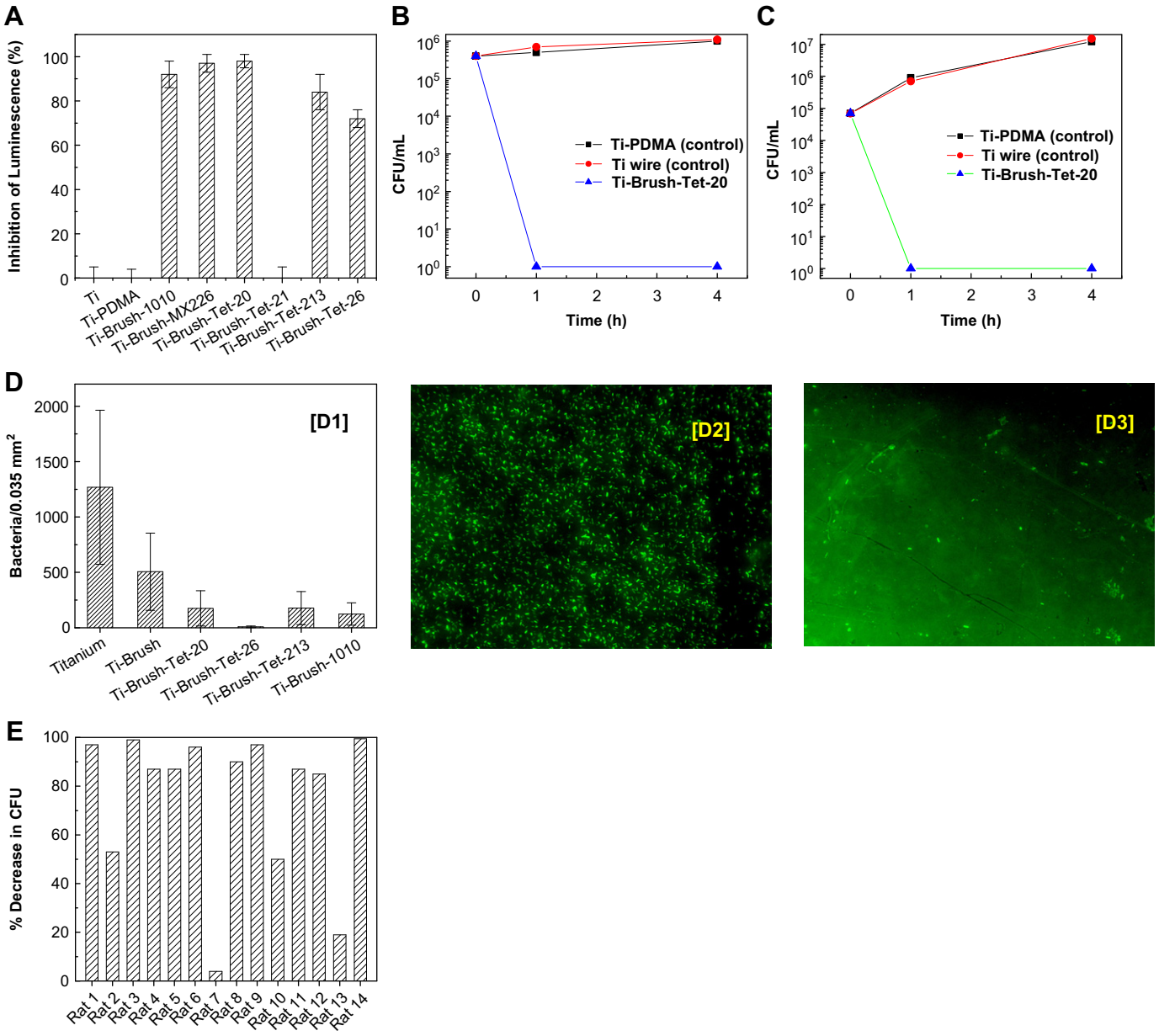


**Fig. 3.** Antimicrobial activity of surface immobilized peptides. [A] Inhibition of luminescence of *P. Arruginosa* upon incubation with titanium slides modified with peptide immobilized copolymer brush (surface area: 1 $cm^2$); inhibition of luminescence is taken as a measure of antimicrobial activity. Ti-slides and polydimethylacrylamide (PDMA) brush coated Ti-slides (neutral brushes) were used as controls. [B] and [C] Antibacterial acitivity of peptide immobilized titanium wire (surface area: 20 $cm^2$, bacteria: [B] *P. arruginosa*, [C] *S. aureus*) as measured by bacteria colony count method. Titanium wire modified with Tet-20 immobilized copolymer brush. Decrease in colony forming unit (CFU) of bacteria is taken as a measure of antimicrobial activity. [D] Comparison of biofilm formation on AMPs conjugated copolymer brushes on titanium surface. Surfaces with and without peptides after 1 week of incubation with *Pseudomonasaeruginosa* in ¼ BHI, magnification 1:600. Bacteria are stained using SYTO 9 (Invitrogen). [D1] Bacteria count on peptide immobilized titanium surfaces. [D2] Fluorescence image of bacteria on titanium surface, [D3] Fluorescence image of bacteria on peptide (Tet-26) immobilized copolymer brush on titanium surface. [E] *In vivo* analysis; percent decrease in the number of bacteria (*S. aureus*) adherent to the Tet-20 immobilized implants compared to the implant without peptides as controls. The implants were placed into the subcutaneous pocket of rat at which 250 μl of approximately $10^8$ bacteria was injected onto the surface of the implant. The wound was closed using 5/0 Vicryl sutures. Bacteria count on the implant was determined after 7 days by surgically removing the implant.

(Enviro Genie by Scientific Industries Inc.) and incubated at 37 °C at 6.12 rotations per minute. The first screen was performed for 1, 2, 3 and 7 days (see Figure 5S, supplementary information), while subsequent experiments were performed after a period of 7 days. After incubation, the Ti-slides were washed and stained with SYTO 9 (Invitrogen) according to the manufacturer's protocol. The density of bacteria attached on uncoated titanium slides after 7 days was very high with 1268 ± 695 bacteria per 0.035 $mm^2$, (Fig. 3D2) and frequently biofilm formation was observed, (Figure 5SD; supplementary information). The best result in inhibiting bacterial attachment was observed for the Tet-26 conjugated copolymer brush surface, with only 8.4 ± 6.6 bacteria per 0.035 $mm^2$ retained (Fig. 2D3). Second best was the peptide Tet-20 (175 ± 158 bacteria per 0.035 $mm^2$; Fig. 3D1). Bacterial adhesion to AMP conjugated brushes was lower than that on the control copolymer brushes which could be attributed to the antimicrobial activity of the AMP conjugated brushes or in part due to the changes in surface properties. However the former is the likely explanation as anionic bacteria would tend to bind more avidly to positively charged surfaces.

Based on its potent antimicrobial activity *in vitro*, Tet-20 conjugated titanium implants were tested in an *in vivo* rat infection model. Tet-20 coated Ti-wires were implanted into subcutaneous pockets made on the dorsal side of rats, and were challenged with $10^8$ CFU of *S. aureus*. Following a 7 day implantation period, the implants were removed and the CFU were determined. In 10 out of 14 rats the CFUs were decreased by at least 85% (Fig. 3E). The results indicated that the conjugation of Tet-20 to titanium implants via a polymer brush linker is an effective way to significantly decrease the number of bacteria adherent to the implants compared to the control sample containing just the PDMA brush without peptides ($p = 0.0426$). This *in vivo* model of implant-associated infections utilized a high infectious concentration of *S. aureus* and provided evidence that the direct antimicrobial activity of the AMP conjugated implants conferred protection against implant-associated infections. In fact a higher number of bacteria was used than the implant would be exposed to in a clinical setting, where contamination of implants generally occurs while the implant is outside the body waiting to be inserted or as a result of brushing up against non-sterile surfaces (e.g. skin) upon implantation [1,2]. Given the effectiveness of these AMP coatings against the high number of bacteria used in this study, it is likely that they would offer more than sufficient antimicrobial activity in a clinical setting where the implants would be exposed to significantly less bacteria and usually in combination with the systemic or local administration of antibiotics.

A lack of hemocompatibility (highly relevant to vascular implants) and increased mammalian cell toxicity were major reasons for the poor performance of previously tested poly cationic as well as some silver-based antimicrobial coatings on implants [7,14,19]. Given the excellent non-specific protein/cell resistant properties of hydrophilic polymer brushes [27,38], we anticipated that the AMP immobilized copolymer brush coating would be non-toxic. To verify this, we tested the hemocompatibility of the Tet-20 conjugated Ti-wire by measuring platelet activation and adhesion, and complement activation in human blood. Approximately 10 $cm^2$ of the Ti-wire was incubated with citrate anticoagulated platelet rich plasma in a shaking platform (40 rpm) at 37 °C and the expression of platelet activation marker CD 62P was measured using fluorescently labeled anti-CD62P antibody [27]. The Tet-20 peptide conjugated implant and the control brush (no peptide) implant did not activate platelets in the solution phase (Fig. 4A), and also did not result in significant platelet adhesion compared to unmodified Ti-wire as evidenced by a scanning electron microscopy (SEM) analysis (Figure 6S supplementary information). This was in contrast to previous investigations of polycat ionic polymer based antimicrobial surfaces [19]. The complement activation in human serum was investigated using a modified CH50 analysis [39]. Complement consumption in human serum upon incubation with AMP conjugated Ti-wire (10 $cm^2$) was measured using sensitized sheep red blood cells. Our results showed that the peptide Tet-20 conjugated surface did not increase complement activation compared to the control serum (Fig. 4B). Taken together, these investigations confirmed the blood compatibility of AMP conjugated polymer brushes. In addition, the cytotoxicity and cell adhesion of three different tethered AMPs (Tet-20, Tet-213 and 1010) were investigated. Ti-slides were chosen as it is difficult to get accurate measurements on Ti-wires due to its high surface roughness. Osteoblast-like cells from human osteosarcoma (MG-63, ATCC® CRL-1427™, USA) were used. Our results showed that the AMP conjugated copolymer brushes did not inhibit cell growth as determined by MTT assays in comparison with control Ti-samples (Fig. 4C). Cell adhesion on the AMP conjugated copolymer brushes on Ti-slides was also measured using SEM analysis after 48 h of incubation (Figure 4D and Figure 7S supplementary information), and showed that the copolymer brush surface (with and without peptides) decreased cell adhesion considerably. AMPs slightly enhanced the cell adhesion compared to the control polymer brush. These results are in agreement with previous work showing that hydrophilic polymer brushes reduce cell adhesion [27,40]. The osteoblast cell adhesion data was consistent with the platelet adhesion and activation on AMP conjugated polymer brushes as well as the bacterial adhesion described above.

To further investigate and correlate the surface properties of AMP conjugated copolymer brushes, the hydrophobic/hydrophilic properties of the copolymer brush surfaces were measured before and after peptide conjugation by means of water contact angle and atomic force microscopy (AFM) force-distance measurements. The water contact angles (Fig. 5A) of AMP-tethered copolymer brushes varied among individual peptides. A range of water contact angles from 37° to 73° were obtained, indicating differences in the hydrophobic character of the surface following AMP conjugation. The adhesion forces between a hydrophobic AFM tip and the AMP-conjugated copolymer brushes were determined and correlated with the contact angle measurements. The maximum adhesive force ($F_H$) between the hydrophobic AFM tip and the peptide conjugated brush surface upon retraction of the AFM tip from the surface was taken as a measure of the hydrophobic interactions [33,41,42]. Results are shown in Fig. 5B. The average values from 50 independent force curves from different spots on the substrate are reported. $F_H$ was obtained from a series of force-distance measurements as demonstrated previously for hydrophilic polymer brushes (see supplementary data for more information, Figure 1S) [33]. We found a direct correlation between the adhesive force and water contact angle of the surfaces, in that surfaces that yielded high adhesive forces also had the highest water contact angles (Fig. 5A and B). The varying degrees of adhesive force and water contact angle between AMPs correlated with the results obtained in the biofilm formation experiments (Fig. 3D1), suggesting that hydrophobic interactions between bacteria and the surface played a major role in the ability of bacteria to form biofilms [2,21]. Results obtained from bacterial adhesion experiments to the varying surfaces further supported this hypothesis. In the present case, peptide conjugated polymer brushes with the lowest adhesive force and water contact angle inhibited biofilm formation the most, as exemplified by Tet-26 (Fig. 5A and B).

It has been suggested previously that the change in conformation of soluble AMPs upon interaction with bacterial membrane and its subsequent incorporation is one mechanism for their antimicrobial activity [43–45]. We investigated whether our end-tethered AMPs interact with model bacterial lipid membranes (DMPC/DMPG) similarly to soluble peptides. The conformation of Tet-20 conjugated to a copolymer brush upon interaction with our model bacterial membrane was measured using oriented CD measurements and compared with the lipid's effects on soluble Tet-20. For this, we synthesized copolymer conjugated Tet-20 on quartz slides (Table 2 and Figure 8S in supplementary information). The CD spectra of Tet-20 (soluble and copolymer brush conjugated) in solutions containing a model bacterial lipid membrane were compared to those obtained in solutions without lipids. The percentage of α-helix conformation of soluble Tet-20 changed from 25% (in PBS) to 92% in the presence of lipid membrane (1:1 DMPC/DMPG at a peptide to lipid ratio of 1:100) (Fig. 5C1). In contrast, the copolymer brush conjugated Tet-20 changed conformation to a substantially lesser degree (Fig. 5C2) (structural content of polymer brush conjugated Tet-20 in PBS: α-helix – 18.6%, β-sheet/strand – 42.3%, β-turn-19.4% and random coil - 19.7% compared to

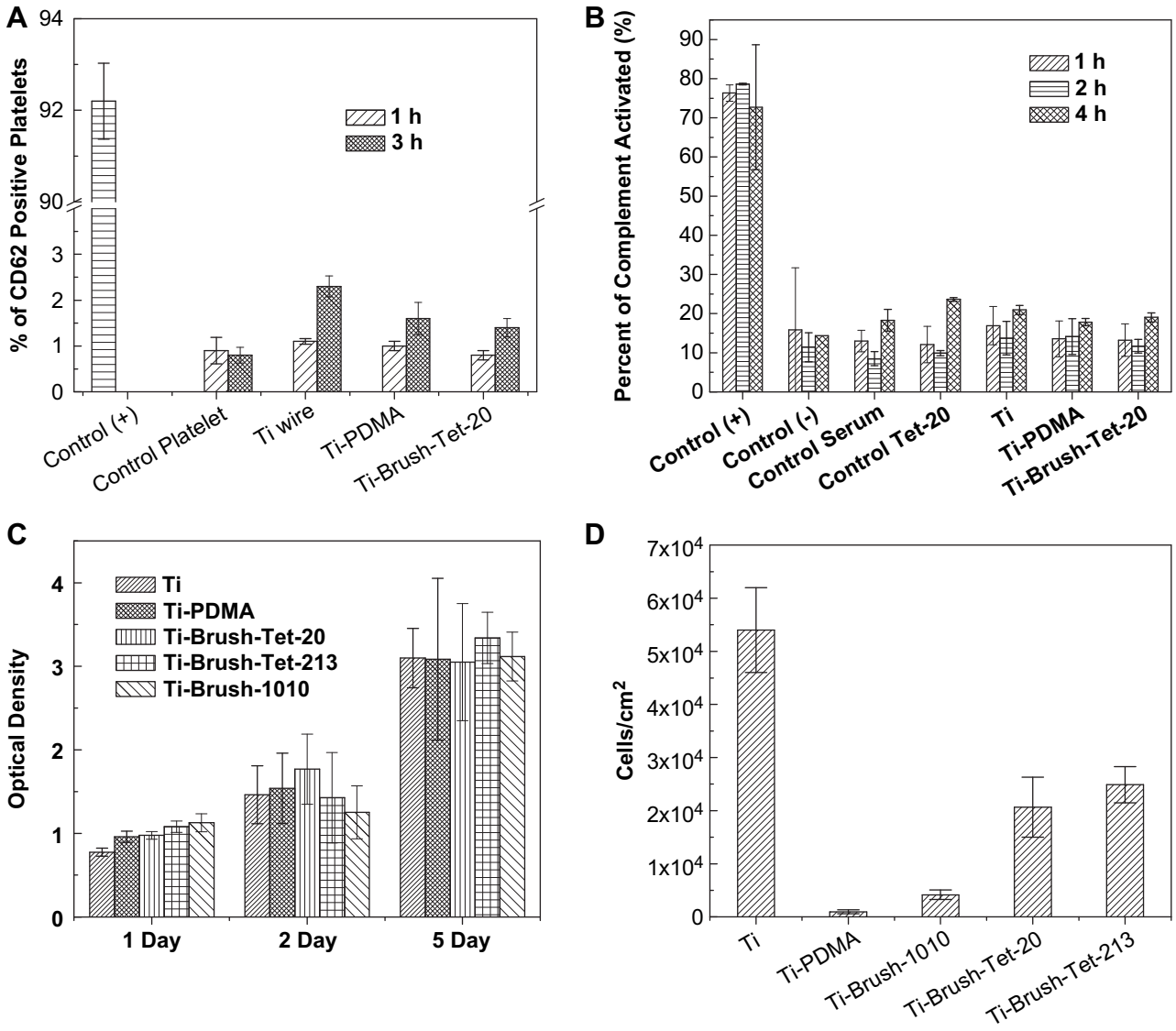


**Fig. 4.** Biocompatibility analysis of peptide immobilized copolymer brush on titanium surface. [A] Effect of peptide (Tet-20) immobilized titanium wire (surface area: 10 $cm^2$) on platelet activation in platelet rich plasma (PRP). Peptide immobilized Ti-wire was placed in PRP at 37 °C for different periods of time in shaking platform and the platelet activation is measured using by flow cytometry. [B] Complement activation by peptide immobilized Ti-wire measured using CH50 analysis. Sensitized sheep erythrocytes were used for measuring the amount of complement proteins consumed during the incubation of implants in serum. Data given are from two technical replicates (average ± SD) and from three different donors. IgG is used as control (+) and EDTA added serum is used as control (−). [C] Effect of peptide immobilized titanium surface (surface area: 1.0 $cm^2$) on cell viability of osteoblast-like cells from human osteosarcoma. Osteoblast-like cells were grown on different AMPs conjugated surface and cell viability is measured using MTT assay. Optical density obtained upon addition of MTT reagent to culture plate is plotted and compared with control samples. There are no significant differences between the control samples and AMPs conjugated samples suggesting the non-toxic behaviour of the peptide coating. [D] Adhesion of osteoblast-like cells on titanium slides conjugated with AMPs measured using scanning electron microscopy measurements. Number of cells adhered on the titanium surface was measured after 48 h.

tethered Tet-20 incubated with lipid membranes: α-helix −52.1%, β-sheet/strand −17.2%,β-turn-10.8% and random coil - 19.1%). The relatively high structural content of Tet-20 immobilized polymer brush observed in the absence of lipid membranes may be due to the presence of the hydrophobic polymer backbone. These results show that the tethered peptides behaved quite differently from soluble peptides, presumably because these short peptides (12 amino acids) were unable to interact efficiently with lipid bilayers when sterically restricted by covalent conjugation to the polymer brush. This is consistent with our previous data demonstrating strong mechanistic difference between tethered and free peptides [25]. Previous results indicated that tethered peptides tend to kill microbes by causing destruction of the bacterial permeability barrier [25]. However, it is unlikely that such tethered 12 amino acid peptides (with a maximal length of 5.5 nm) could reach through the bacterial cell wall peptidoglycan and, for Gram-negative organisms, outer membrane that are 20–80 nm thick to access bacterial cytoplasmic membrane. Rather we have postulated that the disturbance of surface electrostatics must trigger an autolytic and/or cell death mechanism [25]; the studies here indicate that this also involves a conformational change in the peptide. Since the polymer brush immobilization creates a high local density of peptide and positive charge, the method described here represents an ideal way to induce an electrostatic-based mechanism leading to cell death.

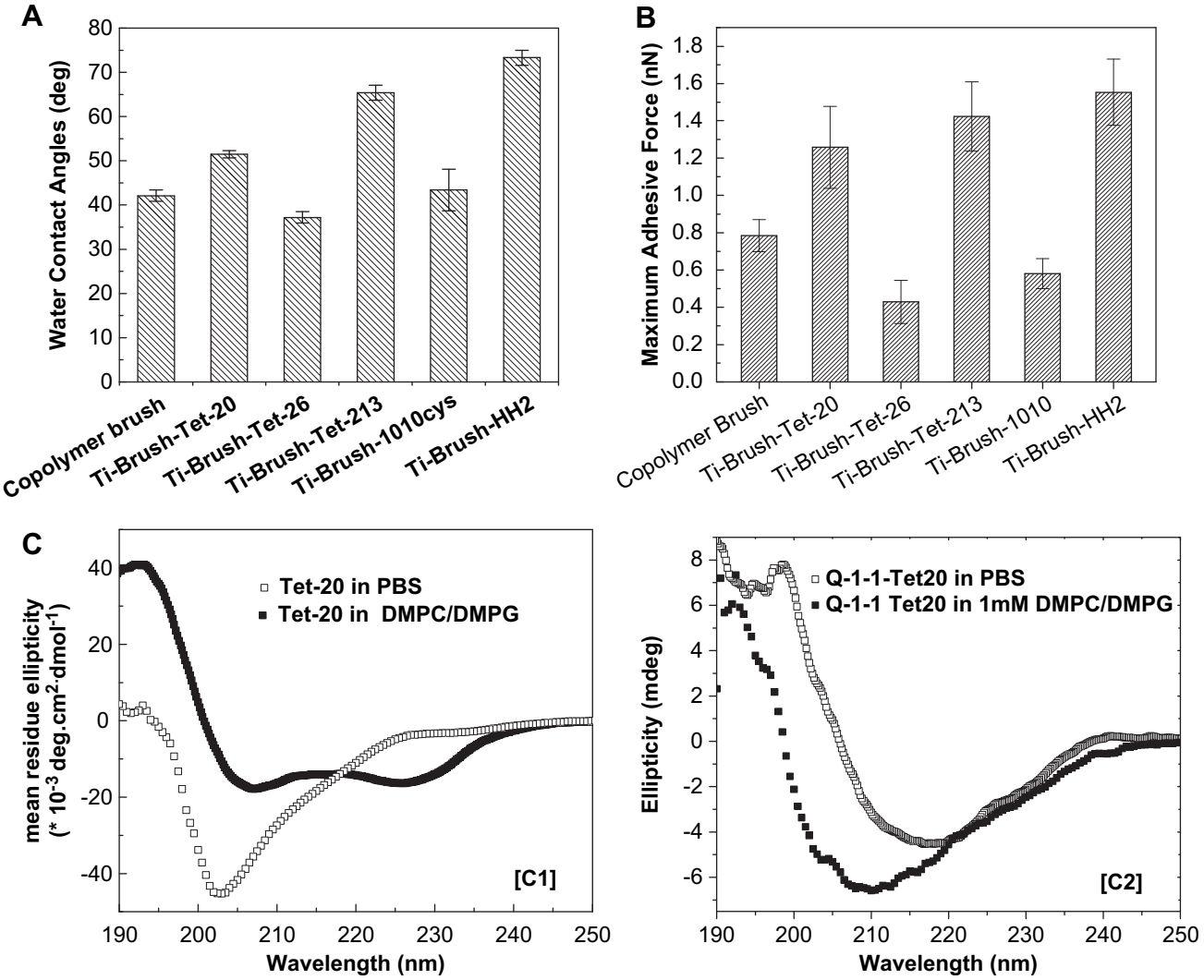


**Fig. 5.** [A] Comparison of water contact angles of different AMPs immobilized copolymer brushes on Ti surface. Graft density of the brushes was constant. PDMA/PAPMA copolymer brush (Table 1) was used as control. [B] Comparison of hydrophobic adhesive forces measured by atomic force microscopy force-distance measurements in water on AMP conjugated copolymer brushes. Maximum adhesive force measured from AFM force-distance curves using silicon nitride tip is given. Graft density of the brushes was constant. PDMA/PAPMA copolymer brush (Table 1) is used as control. [C] Comparison of [C1]CD spectra of AMP Tet-20 in PBS and in presence of model bacterial membrane (DMPC/DMPG, molar ratio: 1/1; peptide/liposome (P/L) molar ratio is 1/100). Bacterial membrane induced conformation changes in the peptide. [C2] Comparison of CD spectra of AMP Tet-20 conjugated copolymer brushes on quartz slides in PBS and in presence of model bacterial membrane (DMPC/DMPG concentration: 1.0 mM). Data show that surface immobilized peptides changed its conformation upon interaction with bacterial lipids.

## 4. Conclusions

We have presented a general method for the development of a biofilm resistant non-toxic hydrophilic polymer coatings having broad spectrum antimicrobial activity on various surfaces. The coatings were prepared by SI-APTRP followed by the conjugation with an optimized series of antimicrobial peptides (AMPs). Surface peptide conjugation depended on the graft density of copolymer brushes and surface concentrations as high as 5.9 $\mu g/cm^2$ was achieved. The polymer brush tethered AMPs showed excellent broad spectrum antimicrobial activity as well as biofilm resistance *in vitro* and it depended on types of AMPs used. The biofilm resistance of the coating was attributed to the combined effect of polymer structure and the presence of AMPs, and the effect was correlated to hydrophobic/hydrophilic character of the coatings. Rat studies demonstrated the ability of the coatings to protect bacterial infection *in vivo*. The AMPs conjugated polymer coatings were non-toxic to mammalian cells, did not activate human platelets or initiated complement activation. The circular dichorism spectroscopy analysis analyses suggesting a different mechanism of action of surface tethered AMPs compared to soluble AMPs. Since polymer brushes can be synthesized on most of the current implant material surfaces, the coating will be widely applicable for compacting implant-associated infections.

## Acknowledgements

This research was supported by a Natural Science and Engineering Council of Canada (NSERC) and by the Canadian Institutes of Health Research (CIHR) through a CHRP grant. Additional funding to REWH from the Advanced Foods and Materials Network are acknowledged. JNK acknowledges New Investigator award from CIHR and Canadian Blood Services (CBS). REWH holds a Canada Research Chair. JK held a postdoctoral fellowship from the Canadian Cystic Fibrosis Foundation. The authors thank the LMB Macromolecular Hub and Spectroscopy Hub at the UBC Centre for Blood

Research for the use of their research facilities, which is supported by the Canadian Foundation for Innovation (CFI) and the Michael Smith Foundation for Health Research (MSFHR). SKS acknowledges funding from NSERC and MSFHR. Authors thank Iren Constantinescu and Benjamin F.L. Lai for technical assistance involving blood compatibility analysis. Po-Ying J. Yeh thanked for the help with Ti deposition on silicon wafer.

## Appendix. Supplementary material

Supplementary data associated with this article can be found, in the online version, at doi:10.1016/j.biomaterials.2011.02.013.

## References

[1] Darouiche RO. Treatment of infections associated with surgical implants. N Engl J Med 2004;350:1422–9.
[2] Darouiche RO. Device – associated infections: a macroproblem that starts with microadherence. Clin Infect Dis 2001;33:1567–72.
[3] Pulcini EL, James G. Biofilms and device implants. In: Paulson DS, editor. Applied biomedical microbiology. Montana: CRC Press; 2009. Ch. 5.
[4] Costerton JW, Stewart PS, Greenberg EP. Bacterial biofilms: a common cause of persistent infections. Science 1999;284:1318–22.
[5] Zimmerli W, Trampuz A, Ochsner PE. Prosthetic–joint infections. N Engl J Med 2004;351:1645–54.
[6] Foxman B. Epidemiology of urinary tract infections: incidence, morbidity, and economic costs. Am J Med 2002;113:5–13.
[7] Matl FD, Obermeier A, Repmann S, Friess W, Stemberger A, Kuehn KD. New anti–infective coatings of medical implants. Antimicrob Agents Chemother 2008;52:1957–63.
[8] Davies D. Understanding biofilm resistance to antibacterial agents. Nat Rev Drug Discov 2003;2:114–22.
[9] Mah TFC, O'Toole GA. Mechanisms of biofilm resistance to antimicrobial agents. Trends Microbiol 2001;9:34–9.
[10] Campoccia D, Montanaro L, Speziale P, Arciola CR. Antibiotic–loaded biomaterials and the risks for the spread of antibiotic resistance following their prophylactic and therapeutic clinical use. Biomaterials 2010;31:6363–77.
[11] Yeh PJ, Hegreness MJ, Aiden AP, Kishony R. Drug interactions and the evolution of antibiotic resistance. Nat Rev Microbiol 2009;7:460–6.
[12] Walsh C. Molecular mechanisms that confer antibacterial drug resistance. Nature 2000;406:775–81.
[13] Hoffman LR, D'Argenio DA, MacCoss MJ, Zhang Z, Jones RA, Miller SI. Aminoglycoside antibiotics induce bacterial biofilm formation. Nature 2005;436:1171–5.
[14] Ramstedt M, Ekstrand–Hammarstrom B, Shchukarev AV, Bucht A, Osterlund L, Welch M, et al. Bacterial and mammalian cell response to poly(3-sulfopropyl methacrylate) brushes loaded with silver halide salts. Biomaterials 2009;30:1524–31.
[15] Sambhy V, MacBride MM, Peterson BR, Sen A. Silver bromide nanoparticle/polymer composites: dual action tunable antimicrobial materials. J Am Chem Soc 2006;128:9798–808.
[16] Hetrick EM, Schoenfisch MH. Reducing imlants–related infections: active release strategies. Chem Soc Rev 2006;35:780–9.
[17] Gollwitzer H, Ibrahim K, Meyer H, Mittelmeier W, Busch R, Stemberger A. Antibacterial poly(d, l-lactic acid) coating of medical implants using a biodegradable drug delivery technology. J Antimicrob Chemother 2003;51:585–91.
[18] Shukla A, Fleming KE, Chuang HK, Chau TM, Loose CR, Stephanopoulos GN, et al. Controlling the release of peptide antimicrobial agents from surfaces. Biomaterials 2010;31:2348–57.
[19] Stevens KN, Knetsch ML, Sen A, Sambhy V, Koole LH. Disruption and activatio of blood platelets in contact with an antimicrobial composite coating consisting of a pyridinium polymer and AgBr. ACS Appl Mater Interfaces 2009;1:2049–54.
[20] Gristina AG. Biomaterial–centered infection: microbial adhesion versus tissue integration. Science 1987;237:1588–95.
[21] Noimark S, Dunnill CW, Wilson M, Parkin IP. The roles of surfaces in catheter–associated infections. Chem Soc Rev 2009;38:3435–48.
[22] Anderson JM, Rodriguez A, Chang DT. Foreign body reaction to biomaterials. Semin Immunol 2008;20:86–100.
[23] Hu WJ, Eaton JW, Ugarova TP, Tang L. Molecular basis of biomaterial–mediated foreign body reactions. Blood 2001;98:1231–8.
[24] Hilpert K, Volkmer–Engert R, Walter T, Hancock REW. High–throughput generation of small antibacterial peptides with improved activity. Nat Biotech 2005;23:1008–12.
[25] Hilpert K, Elliott M, Jenssen H, Kindrachuk J, Fjell CD, Koerner J, et al. Screening and characterization of surface–tethered cationic peptides for antimicrobial activity. Chem Biol 2009;16:58–69.
[26] Hancock REW, Sahl HG. Antimicrobial and host–defense peptides as new anti–infective therapeutic strategies. Nat Biotechol 2006;24:1551–7.
[27] Lai BFL, Creagh AL, Janzen J, Haynes CA, Brooks DE, Kizhakkedathu JN. The inductio of thrombus generation on nanostructured neutral polymer brush surfaces. Biomaterials 2010;31:6710–8.
[28] Xiao SJ, Textor M, Spencer ND, Wieland M, Keller B, Sigrist H. Immobilization of the cell–adhesive peptide Arg–Gly–Asp–Cys (RDGC) on titanium surfaces by covalent chemical attachment. J Mater Sci Mater Med 1997;8:867–72.
[29] Zou Y, Kizhakkedathu JN, Brooks DE. Surface modification of polyvinyl chloride sheets via growth of hydrophilic polymer brushes. Macromolecules 2009;42:3258–68.
[30] Kizhakkedathu JN, Norris–Jones R, Brooks DE. Synthesis of well–defined environmentally responsive polymer brushes by aqueous ATRP. Macromolecules 2004;37:734–43.
[31] Kizhakkedathu JN, Brooks DE. Synthesis of poly(N, N–dimethylacrylamide) brushes from charged polymeric surfaces by aqueous ATRP: effect of surface initiator concentration. Macromolecules 2003;36:591–8.
[32] Wu T, Efimenko K, Vlcek P, Subr V, Genzer J. Formation and properties of anchored polymers with a gradual variation of grafting densities on flat substrates. Macromolecules 2003;36:2448–53.
[33] Zou Y, Rossi NAA, Kizhakkedathu JN, Brooks DE. Barrier capacity of hydrophilic polymer brushes to prevent hydrophobic interactions: effect of graft density and hydrophilicity. Macromolecules 2009;42:4817–28.
[34] Florin EL, Rief M, Lehmann H, Ludwig M, Dornmair C, Moy VT, et al. Sensing specific molecular interactions with the atomic force microscope. Biosens Bioelecron 1995;10:895–901.
[35] Wang M, Cao Y, Li HB. The unfolding and folding dynamics of TNFnALL probed by single molecule force–ramp spectroscopy. Polymer 2006;47:2548–54.
[36] Ducker WA, Sendan TJ, Pashley RM. Measurement of forces in liquids using a force microscope. Langmuir 1992;8:1831–6.
[37] Lu S. Immobilization of antimicrobial peptides onto titanium surfaces. Univ British Columbia; 2009, MASc. Thesis.
[38] Hucknall A, Rangarajan S, Chilkoti A. In pursuit of zero: polymer brushes that resist the adsorptionof proteins. Adv Mater 2009;21:2441–6.
[39] Bradley AJ, Devine DV, Ansell SM, Janzen J, Brooks DE. Inhibition of liposome–induced complement activation by incorporated polyethylene glycol–lipids. Arch Biochem Biophys 1998;357:185–94.
[40] Wischerhoff E, Uhlig K, Lankenau A, Porner HG, Laschewsky A, Duschl C, et al. Controlled cell adhesion PEG–based switchable surfaces. Angew Chem Int Ed Engl 2008;47:5666–8.
[41] Meyer EE, Rosenberg KJ, Israelachvili J. Recent progress in understanding hydrophobic interactions. Proc Natl Acad Sci USA 2006;103:15739–46.
[42] Geisler M, Pirzer T, Ackerschott C, Lud S, Garrido J, Scheibel T, et al. Hydrophobic and Hofmeister effects on the adhesion of spider silk proteins onto solid substrates: an AFM–based single–molecule study. Langmuir 2008;24:1350–5.
[43] Jelokhani–Niaraki M, Prenner EJ, Kay CM, McElhaney RN, Hodges RS. Conformation and interaction of the cyclic cationic antimicrobial peptides in lipid bilayers. J Pept Res 2002;60:23–36.
[44] Resende JM, Moraes CM, Munhoz VH, Aisenbrey C, Verly RM, Bertani P, et al. Membrane structure and conformational changes of the antibiotic heterodimeric peptide distinction by solid–state NMR spectroscopy. Proc Natl Acad Sci USA 2009;106:16639–44.
[45] Wieczorek M, Jenssen H, Kindrachuk J, Scott WR, Elliott M, Hilpert K, et al. Structureal studies of a peptide with immune modulating and direct antimicrobial activity. Chem Biol 2010;17:970–80.